



Fracture mechanics modeling of popping event during daughter cell separation

Yuxuan Jiang^{1,2} · Xudong Liang¹ · Ming Guo³ · Yanping Cao² · Shengqiang Cai¹

Received: 24 January 2018 / Accepted: 23 April 2018
© Springer-Verlag GmbH Germany, part of Springer Nature 2018

Abstract

Most bacteria cells divide by binary fission which is part of a bacteria cell cycle and requires tight regulations and precise coordination. Fast separation of *Staphylococcus Aureus* (*S. Aureus*) daughter cells, named as popping event, has been observed in recent experiments. The popping event was proposed to be driven by mechanical crack propagation in the peripheral ring which connected two daughter cells before their separation. It has also been shown that after the fast separation, a small portion of the peripheral ring was left as a hinge. In the article, we develop a fracture mechanics model for the crack growth in the peripheral ring during *S. Aureus* daughter cell separation. In particular, using finite element analysis, we calculate the energy release rate associated with the crack growth in the peripheral ring, when daughter cells are inflated by a uniform turgor pressure inside. Our results show that with a fixed inflation of daughter cells, the energy release rate depends on the crack length non-monotonically. The energy release rate reaches a maximum value for a crack of an intermediate length. The non-monotonic relationship between the energy release rate and crack length clearly indicates that the crack propagation in the peripheral ring can be unstable. The computed energy release rate as a function of crack length can also be used to explain the existence of a small portion of peripheral ring remained as hinge after the popping event.

Keywords Cell division · Daughter cell separation · Fracture · Crack propagation · Popping

1 Introduction

Crack propagation-driven popping phenomena can be widely seen in plants and fungi. For instance, the seedpod of jewelweed can effectively discharge the seeds to a long distance through popping event which is known to be driven by fast crack growth between the valves (Sakes et al. 2016). As another example, sporangium of *Pilobolus* (a genus of fungi)

can suddenly break from the sporangiophore and be propelled forward by cell sap jet (Sakes et al. 2016). Interestingly, moreover, recent experimental studies on *Staphylococcus Aureus* (*S. Aureus*) cells revealed that its daughter cell separation may be also through crack propagation-driven popping event (Zhou et al. 2015, 2016). The breakage of the peripheral ring during daughter cell separation has shown to be completed within several milliseconds in the experiments. Such a rapid separation of *S. Aureus* daughter cells with no detectable intermediate stages (Tzagoloff and Novick 1977; Zhou et al. 2015, 2016) is in direct contrast to gradual morphological changes often observed during division of other bacteria or eukaryotic cells (Egan and Vollmer 2013). It was proposed that such fast separation of *S. Aureus* daughter cells might be driven by mechanical crack propagation in the peripheral ring (Zhou et al. 2015, 2016), and a large stress might be generated in the peripheral ring during the inflation of daughter cells (Zhou et al. 2015).

While the computation of stress field can provide important insights into the failure of biological materials, the model based on fracture mechanics theory is necessary to fully understand crack propagation in those biological processes

Yuxuan Jiang and Xudong Liang have contributed equally to this work.

✉ Shengqiang Cai
shqcai@ucsd.edu

¹ Department of Mechanical and Aerospace Engineering, University of California, San Diego, La Jolla, CA 92093, USA

² Department of Engineering Mechanics, Institute of Biomechanics and Medical Engineering, Tsinghua University, Beijing 100084, People's Republic of China

³ Department of Mechanical Engineering, Massachusetts Institute of Technology, Cambridge, MA 02139, USA

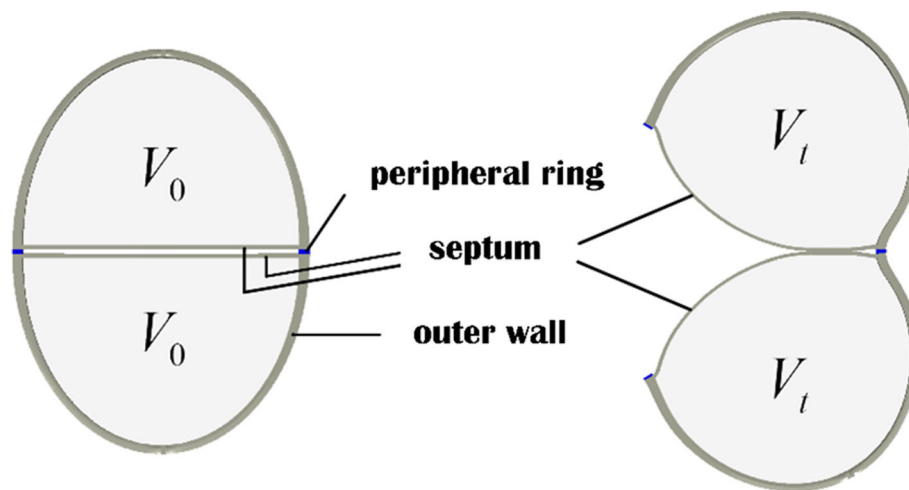


Fig. 1 Schematics of *S. Aureus* daughter cell separation, recapping the main observation of a recent experiment (Zhou et al. 2015). A peripheral ring connects two daughter cells before separation. When the two daughter cells are inflated large enough, fast separation or so-called popping event is observed in the experiments (Zhou et al. 2015). After

the fast separation, a small portion of the peripheral ring is remained as a hinge connecting the two daughter cells. Three major components of the cell structure are highlighted and are considered in the model: the outer wall, the septum and the peripheral ring. V_0 and V_t are the volumes of the daughter cells before and after inflation, respectively

discussed above. It is well known that crack growth is often initiated from existing defects. However, it is practically difficult, if possible, to predict the magnitude of stress and strain near a defect with an irregular shape (Griffith 1921). Instead, on the basis of fracture mechanics theory, the critical condition for a crack to grow (namely, the energy release rate being equal to the fracture toughness of the material) has been validated in numerous experiments (Anderson 2017). In addition, under certain loading conditions, whether a crack propagates stably or unstably can only be understood based on fracture mechanics theory (Hutchinson and Paris 1979).

In this article, we develop a fracture mechanics model for the breakage of peripheral ring during *S. Aureus* daughter cell separation. By using finite element analysis, we calculate the energy release rate associated with the crack growth in the peripheral ring, when daughter cells are inflated by a uniform turgor pressure. Although the cell separation reported in the experiment is fast dynamic process, our fracture mechanics model is quasi-static, considering that the crack propagation speed ($\sim 1\text{mm/s}$) is still far below the sound speed of the material and thus the material inertia has negligible effects. Our results show that with a fixed volume growth of the inflated cells, when the crack is short, the energy release rate increases with the increase in crack length. The energy release rate reaches a maximum value when the crack is of an intermediate length and then decreases with further increase in crack length. Such a non-monotonic change of energy release rate with crack length can be used to explain the fast crack propagation and the subsequent crack arrest observed in the experiments (Zhou et al. 2015, 2016).

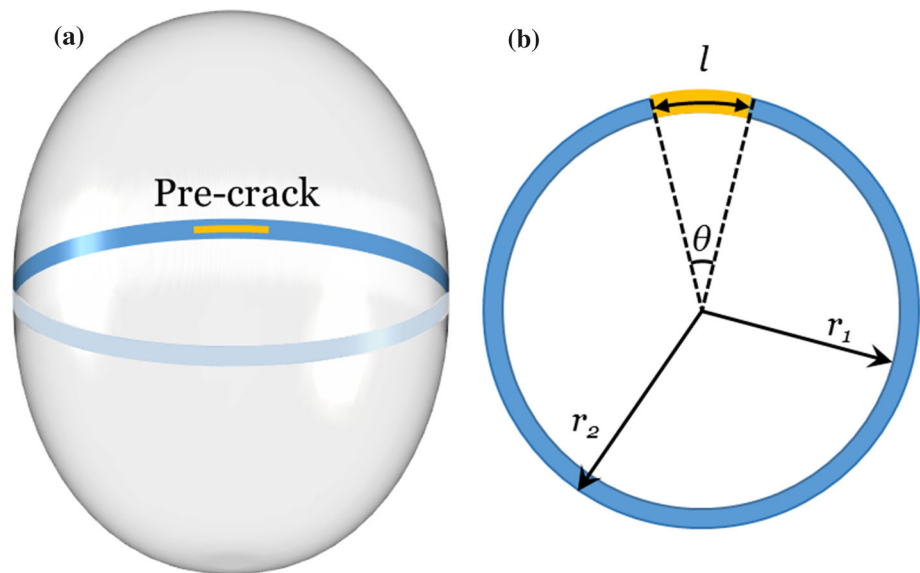
2 Modeling of the fracture of the peripheral ring during *S. Aureus* daughter cell separation

2.1 Mechanical model of cell

We construct mechanical models of *S. Aureus* to determine the deformation and stress distribution accompanying with the growth and “popping” event during the daughter cell separation. The cell structure in our model is composed of three major components—the outer wall, the septum and the peripheral ring (Fig. 1). The *S. Aureus* cell prior to the “popping” event is modeled as a prolate ellipsoid in accord with the experimental observations (Matias and Beveridge 2007; Zhou et al. 2015). The septa are two parallel plates in the middle of the cell, which separate one cell to two hemispherical daughter cells. One daughter cell is composed of one outer wall and one septum, connected by a peripheral ring to the other before cell separation. For simplicity, we assume that both the septum and the peripheral ring are circular with the same radius. The outer cell wall, the septum and the peripheral ring are assumed to be composed of the same isotropic, incompressible, hyperelastic material, whose constitutive relationship can be given by the Neo-Hookean model (Treloar 1975). The geometrical parameters of the model are selected based on the studies of *S. Aureus* cell division (Zhou et al. 2015). Details of the parameters adopted in the mechanical model are given in “Appendix.”

After the formation of septum during the *S. Aureus* cell division, the volume of each daughter cell continues to grow exponentially with time (Godin 2010; Zhou et al. 2015),

Fig. 2 **a** Peripheral ring with a pre-crack before the inflation of daughter cells. Blue region refers to the peripheral ring and yellow region refers to the pre-crack. **b** Top view of a crack in the peripheral ring. The crack length is measured by its central angle $\theta = l/r_2$. The inner and outer radius of the peripheral ring before cell inflation is r_1 and r_2 , respectively



while the peripheral ring does not grow as much as the rest of the cell, which leads to substantial mechanical stresses developed in the peripheral ring before cell separation. In this model, we assume that the peripheral ring does not grow after the septum formation, and the volume growth of the daughter cell can be depicted by the volume growth ratio defined as,

$$\eta = \frac{V_t}{V_0} \quad (1)$$

where V_0 and V_t are the volume of the daughter cell immediately after the septum formation and after the inflation of daughter cells, respectively. In the experiments (Zhou et al. 2015), it was shown that the volume of the inflated daughter cells was almost unchanged during the fast crack propagation in the peripheral ring. Therefore, the loading parameter–volume growth ratio η is assumed to be unchanged during the crack propagation in our following calculations. When the volume growth ratio is small, the peripheral ring is stressed without inducing the growth of crack. When η is large, crack propagates in the peripheral ring and can induce popping phenomenon observed in the experiments (Zhou et al. 2015, 2016).

2.2 Fracture mechanics modeling of cell separation

We develop a fracture mechanics model to study crack growth in the peripheral ring during *S. Aureus* daughter cell separation. Based on the theory of fracture mechanics (Anderson 2017), we calculate energy release rate G associated with growth of crack in peripheral ring as a function of the volume growth ratio η . In order to calculate the energy release rate, we first introduce a pre-crack in the peripheral ring with

length l as shown in Fig. 2. The energy release rate is defined as:

$$G = \frac{dW(S, \eta)}{dS} \quad (2)$$

where $W(S, \eta)$ is the strain energy stored in the cellular structure and S is the area of crack surface.

Energy release rate can be regarded as the driving force for crack growth. The key assumption in fracture mechanics is when the energy release rate reaches the fracture toughness of the material, a crack begins to grow. Scaling analysis enables us to write the energy release rate in the following dimensionless form,

$$G = \mu r_2 f(\theta, \eta) \quad (3)$$

where μ is the shear modulus of the material, r_2 is the outer radius of the peripheral ring after the formation of septum (Fig. 2b). The dimensionless function $f(\theta, \eta)$ needs to be calculated, and θ is central angle of an arc crack defined as $\theta = l/r_2$ as shown in Fig. 2b.

In this article, we compute the normalized energy release rate $f(\theta, \eta)$ using finite element analysis software, ABAQUS. To calculate the energy release rate, cracks of different lengths are introduced in the peripheral ring in the finite element models as shown in Fig. 2a. The central angle of a crack ranges from 0 to 2π . By prescribing the cell volume growth ratio of the daughter cell, we can numerically compute the energy release rate as a function of the crack length. We model a prolate ellipsoidal cell discretized in a three-dimensional hexahedral mesh with approximately 1,300,000 nodes and approximately 250,000 quadratic reduced hexahedral elements (C3D20R). Mesh around the crack tip is significantly refined. Spatial (grid) convergence has been ver-

ified by refining mesh. The finite element model is based on the geometry provided in Fig. 7. The volume growth in each daughter cell is realized by using “fluid cavity” technique in ABAQUS. In the simulations, we fill incompressible fluid in each daughter cell and control the volume growth of each daughter cell through thermal expansion of the fluid. As a consequence, we can precisely control the volume growth ratio of the daughter cell by varying the temperature of the fluid.

With prescribing both of the crack length and the volume growth ratio, we conduct the finite element simulations using ABAQUS/Standard. We assume the contact between the two daughter cells is frictionless during the cell separation. The adhesion between the daughter cells is also neglected in the current study. According to Eq. (3), the energy release rate can be obtained through computing the difference between the elastic strain energy of the cell with crack length l and $l + \Delta l$, where Δl is a small increment of the crack length. We use a PYTHON script to calculate the energy release rate with different crack lengths automatically.

3 Results

3.1 Energy release rate during daughter cell separation

In Fig. 3, we plot the normalized energy release rate $f(\theta, \eta)$ with respect to the central angle of the crack under different volume growth ratios ranging from 1.0 to 1.27. The maximal volume growth ratio, 1.27, corresponds to the one observed in the experiments with fast crack propagation in the peripheral ring (Zhou et al. 2015). As shown in Fig. 3, when the crack is short, the elastic strain energy stored in the cellular structure does not change significantly with the change of the crack length, and energy release rate is small. When the crack is long, the stress in the peripheral ring is almost fully relaxed, and the energy release rate is also small. The energy release rate reaches the maximal value when the crack is of an intermediate length, which is around π for its central angle as η varying from 1.0 to 1.27 (Fig. 3). We have also confirmed that the energy release rate calculated from Eq. (3) is very close to the number obtained by J-integral around the crack tip also obtained from finite element simulations (Fig. 4). It is noted that we calculate the energy release rate based on quasi-static models by neglecting the inertial effect, given the fact that the crack propagation speed ($\sim 1\text{mm/s}$) is much slower than the sound speed.

The maximum normalized energy release rate (f^*) only depends on the cell volume growth ratio. The values of f^* can be fitted to the following polynomial function of the cell volume growth ratio,

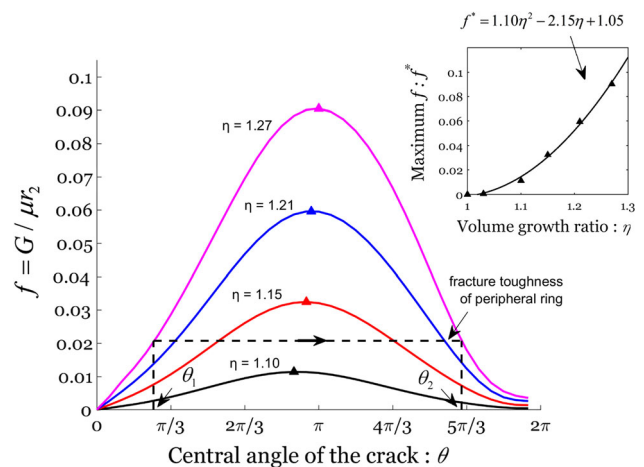


Fig. 3 Normalized energy release rate f versus central angle of the crack θ for different volume growth ratios. For a fixed crack length, energy release rate increases with the increase in volume growth ratio. For a fixed volume growth ratio, energy release rate first increases and then decreases with the increase in crack length. Such non-monotonic relationship predicts unstable crack growth and crack arrest in the peripheral ring, which is consistent with the experimental observation (Zhou et al. 2015). For example, the central angle of the pre-crack in the peripheral ring is θ_1 , and the fracture toughness of the ring is given by the horizontal dash line. When the volume growth ratio reaches $\eta = 1.27$, the crack begins to grow spontaneously till the energy release rate decreases to the fracture toughness of the ring with the central angle of the crack θ_2 . The dependence of maximal normalized energy release rate f^* (marked with triangles) on the volume growth ratio is shown in the inset.

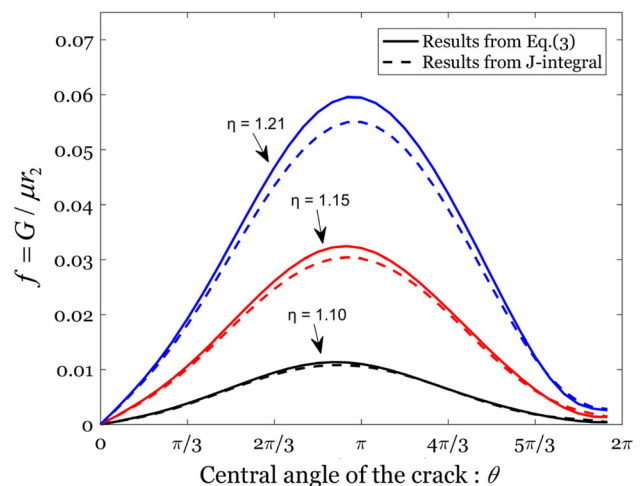


Fig. 4 Comparison between the energy release rate calculated from Eq. (3) and the J-integral. Solid lines represent normalized energy release rate f from Eq. (3). Dash lines represent the normalized J-integral results

$$f^* = 1.10\eta^2 - 2.15\eta + 1.05 \tag{4}$$

where η is in the range of 1.0–1.27. We plot the maximum normalized energy release rate as a function of the volume growth ratio in the inset of Fig. 3. When the maximum energy

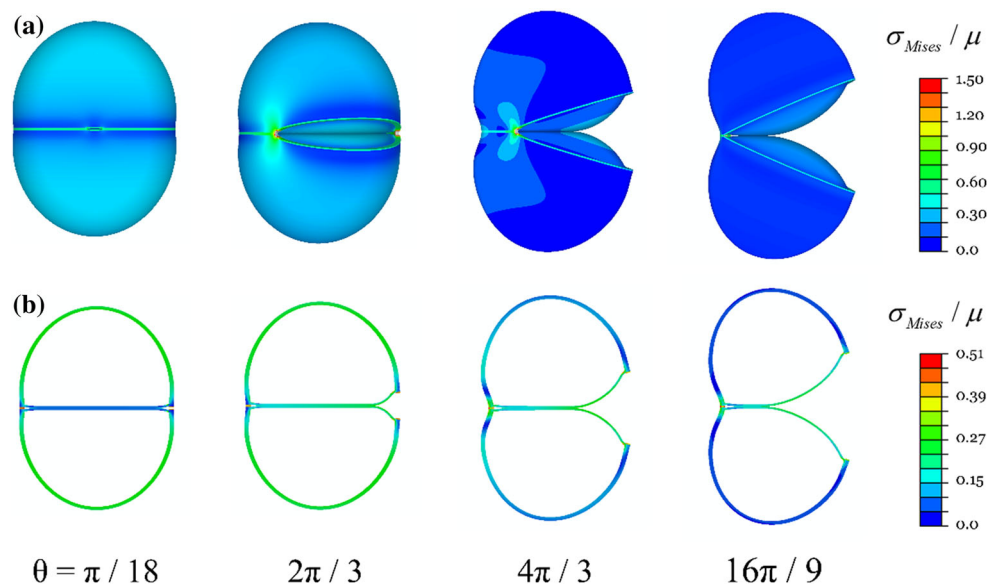


Fig. 5 Finite element simulations of the daughter cell separation with the central angle of the crack in the peripheral ring increased from $\pi / 18$ to $16 \pi / 9$, for a constant volume growth ratio $\eta = 1.21$. **a** The shape

of the cell. **b** The shape of one symmetric cross section of the cell. The color stands for the normalized von Mises stress

release rate is smaller than the fracture toughness of the peripheral ring, crack growth cannot happen even with a large pre-crack in the peripheral ring.

As observed in the experiments (Touhami et al. 2004; Zhou et al. 2015), multiple holes can exist in the peripheral ring. Single hole or coalescence of several holes can form pre-cracks in the peripheral ring. With the increase in volume growth ratio, for a fixed length of pre-crack, energy release rate increases. Once the energy release rate reaches the fracture toughness of the peripheral ring, crack begins to propagate. Considering the small size of a single hole (typically around 100 nm and much smaller than the radius of the peripheral ring), the central angle of the pre-crack should be much smaller than π . Therefore, with a fixed volume growth ratio, energy release rate first increases with the increase in crack length and then decreases, as shown in Fig. 3. This result indicates that once the crack begins to grow, the crack can grow spontaneously without requiring further increase in volume growth ratio till the energy release rate decreases to be equal to the fracture toughness of the peripheral ring again (Fig. 3). It is noted that in the above discussion, we assume a constant fracture toughness of the peripheral ring during the crack propagation. In another word, we assume the R-curve (Anderson 2017) of the peripheral ring is a step-like function as shown in the dashed line in Fig. 3. A precise shape of R-curve is needed to quantitatively predict the unstable crack growth phenomenon.

For a given volume growth ratio, crack growth can be arrested when the energy release rate decreases to the fracture toughness of the peripheral ring with large crack length,

which is consistent with the observation of a remained hinge connecting two daughter cells after the popping event. In Fig. 5, we plot the FEM simulations of the shape of separated daughter cells with different crack lengths under the volume growth ratio $\eta = 1.21$. The three-dimensional deformation and stress distribution during the daughter cell separation are shown in Fig. 5a. With the increase in the crack length, the septa bulge out of plane, contact with each other and push the two daughter cells away from each other. Stress is concentrated near the crack tip. In Fig. 5b, we show the shapes of one symmetric cross section of daughter cells. When the crack length is small, the outer wall of the cells is under high turgor pressure. As the crack length increases, the deformation in the septum increases and pushes the two daughter cells away from each other.

3.2 Pre-stretch analysis

In the previous analysis, the peripheral ring is assumed to be stress-free before the volume growth of the daughter cells. However, as shown in the experiments (Zhou et al. 2015), the peripheral ring can be stretched in the circumferential direction to match the size of the cell during the septum formation. Therefore, we next investigate the effect of the pre-stretch in the peripheral ring on the crack growth. We assume the peripheral ring is pre-stretched in the hoop direction before the inflation of daughter cells. Based on the Neo-Hookean model, the hoop stress $\sigma_{\theta\theta}$ can be calculated as,

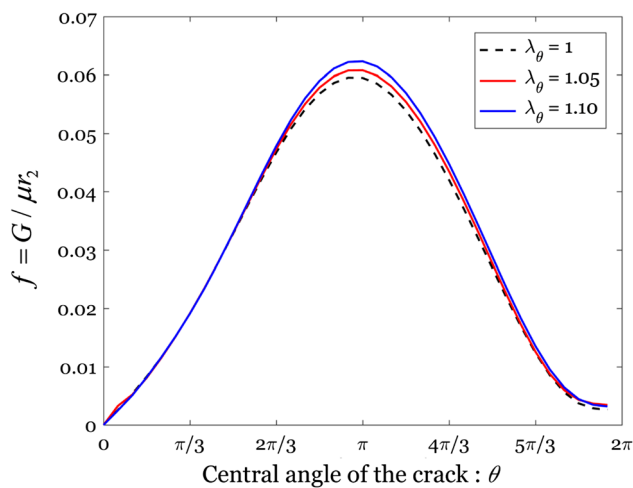


Fig. 6 Normalized energy release rate versus central angle of the crack for different pre-stretches in the hoop direction of the peripheral ring, with the volume growth ratio $\eta = 1.21$

$$\sigma_{\theta\theta} = \mu \left(\lambda_{\theta}^2 - 1/\lambda_{\theta} \right) \quad (5)$$

The pre-stretch in the hoop direction λ_{θ} has been reported to be between 1 and 1.1 in the experiments (Zhou et al. 2015). In the simulation, we set the pre-stretch in the hoop direction to be 1, 1.05 and 1.1. By incorporating corresponding initial stresses in the peripheral ring into the finite element simulations, we obtain the energy release rate associated with crack growth with a volume growth ratio of $\eta = 1.21$, as shown in Fig. 6. The existence of the pre-stretch does not change the shape of the function of the energy release rate too much, though it can cause small quantitative changes; for example, for the case shown in Fig. 6, such quantitative changes are within 5%. Therefore, we conclude that the pre-stretch in the peripheral ring may not be critical for the popping event during daughter cell separation.

4 Conclusion

In this article, we develop a fracture mechanics model to explain recent experimental observation of the popping event during division of *S. Aureus* cell. We show that the energy release rate associated with the crack growth in the peripheral ring depends on the crack length in a non-monotonic way. When the crack is short, the energy release rate is small and increases with the crack length. The energy release rate reaches a maximum value for the crack of an intermediate length and decreases with further increase of crack length. Such a non-monotonic relationship between energy release rate and crack length can be readily used to explain the unstable and fast crack growth as well as crack arrest in the peripheral ring reported in the recent experiments. The frac-

ture mechanics model developed in the article to explain the crack propagation-driven popping event in *S. Aureus* daughter cell separation can be easily generalized to understand other popping events driven by crack propagation, such as those observed in various plants and fungi mentioned at the beginning of the article. At last, we are thankful to one of the anonymous reviewers for pointing out that the cohesive zone model (Gao and Gao 2016; Liu and Gao 2015) may be a better choice for quantitative understanding fracture phenomena in cells. We believe the elastic fracture mechanics model developed in this article provides a mechanism which links the “popping” event of the cell and unstable crack growth in the peripheral ring.

Acknowledgements S.C. acknowledges the support from Hellman Fellows Fund. Y.J. and Y.P.C. acknowledge the support from the National Natural Science Foundation of China (Grant Nos. 11572179, 11432008) and Tsinghua National Laboratory for Information Science and Technology.

Compliance with ethical standards

Conflict of interest The authors declare that they have no conflict of interest.

Appendix: Geometry and material parameters

Figure 7 shows the geometry of the model of a quarter of a cell directly obtained from previous study (Zhou et al. 2015).

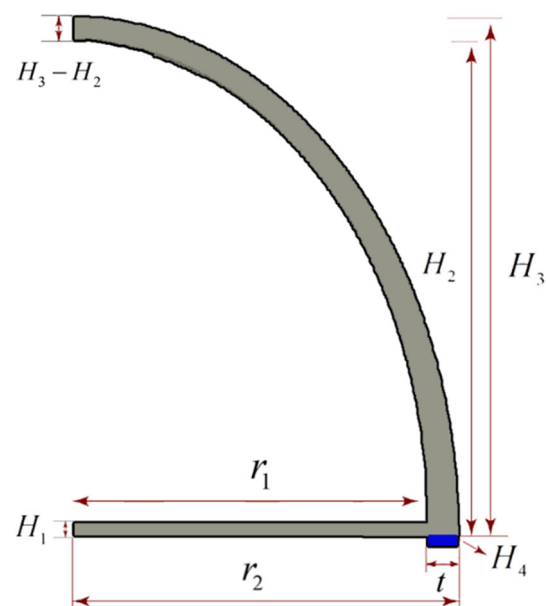


Fig. 7 Geometry of the mechanics model of a quarter of a cell

Table 1 Material and geometrical parameters used in the mechanics model

Parameter	Description	Value (dimensionless)	Rationale
Material parameters			
E	Young's modulus	1	Non-dimensionalization
ν	Poisson ratio	0.49	Incompressible material
μ	Shear modulus	0.3356	$\mu = \frac{E}{2(1+\nu)}$
C_{10}	Neo-Hookean parameter	0.1678	$C_{10} = \frac{E}{4(1+\nu)}$
D_1	Neo-Hookean parameter	0.12	$D_1 = \frac{6(1-2\nu)}{E}$
Geometrical parameters			
H_1	Height of the septum	0.0342	Non-dimensionalization
H_2	Inner length of major axis of the cell	1.4265	Non-dimensionalization
H_3	Outer length of major axis of the cell	1.4835	Non-dimensionalization
H_4	Height of the ring	0.033	Non-dimensionalization
R_0^*	Radius of the ring (before septum formation)	1	Non-dimensionalization
r_1	Inner radius of the ring (after septum formation)	1.071	Non-dimensionalization
r_2	Outer radius of the ring (after septum formation)	1.15	Non-dimensionalization
t	Thickness of the ring (after septum formation)	0.079	$t = r_2 - r_1$

* R_0 is the radius of the peripheral ring before the septum formation, which is not shown in Fig. 7 and is adopted to normalize the other length scales in the cell

Table 1 includes all geometrical and material parameters used in simulations.

References

- Anderson TL (2017) Fracture mechanics: fundamentals and applications. CRC Press, Boca Raton
- Egan AJ, Vollmer W (2013) The physiology of bacterial cell division. *Ann N Y Acad Sci* 1277:8–28
- Gao Z, Gao Y (2016) Why do receptor-ligand bonds in cell adhesion cluster into discrete focal-adhesion sites? *J Mech Phys Solids* 95:557–574
- Godin M et al (2010) Using buoyant mass to measure the growth of single cells. *Nat Methods* 7:387–390
- Griffith AA (1921) The phenomena of rupture and flow in solids. *Phil Trans R Soc Lond A* 221:163–198
- Hutchinson J, Paris P (1979) Stability analysis of J-controlled crack growth. Elastic-plastic fracture. *ASTM STP* 668:37–64
- Liu Y, Gao Y (2015) Non-uniform breaking of molecular bonds, peripheral morphology and releasable adhesion by elastic anisotropy in bio-adhesive contacts. *J R Soc Interface* 12:20141042
- Matias VR, Beveridge TJ (2007) Cryo-electron microscopy of cell division in *Staphylococcus aureus* reveals a mid-zone between nascent cross walls. *Mol Microbiol* 64:195–206
- Sakes A, van der Wiel M, Henselmans PW, van Leeuwen JL, Dodou D, Breedveld P (2016) PLoS ONE. Shooting mechanisms in nature: a systematic review 11:e0158277
- Touhami A, Jericho MH, Beveridge TJ (2004) Atomic force microscopy of cell growth and division in *Staphylococcus aureus*. *J Bacteriol* 186:3286–3295
- Treloar LRG (1975) The physics of rubber elasticity. Oxford University Press, Oxford
- Tzagoloff H, Novick R (1977) Geometry of cell division in *Staphylococcus aureus*. *J Bacteriol* 129:343–350
- Zhou X, Halladin DK, Rojas ER, Koslover EF, Lee TK, Huang KC, Theriot JA (2015) Mechanical crack propagation drives millisecond daughter cell separation in *Staphylococcus aureus*. *Science* 348:574–578
- Zhou X, Halladin DK, Theriot JA (2016) Fast mechanically driven daughter cell separation is widespread in actinobacteria. *mBio* 7:e00952-16

Publisher's Note Springer Nature remains neutral with regard to jurisdictional claims in published maps and institutional affiliations.